Geophysical Journal International



doi: 10.1093/gji/ggz234

Geophys. J. Int. (2019) 218, 1428–1441 Advance Access publication 2019 May 17 GJI Geomagnetism, rock magnetism and palaeomagnetism

Anisotropy of (partial) isothermal remanent magnetization: DC-field-dependence and additivity

Andrea R. Biedermann, 1,2 Mike Jackson, 1 Dario Bilardello 1 and Joshua M. Feinberg 1

¹Institute for Rock Magnetism, University of Minnesota, 55455 Minneapolis, MN, USA. E-mail: andrea.regina.biedermann@gmail.com

²Institute of Geological Sciences, University of Bern, 3012 Bern, Switzerland

Accepted 2019 May 16. Received 2019 May 10; in original form 2019 March 11

SUMMARY

Anisotropy of isothermal remanent magnetization (AIRM) is useful for describing the fabrics of high-coercivity grains, or alternatively, the fabrics of all remanence-carrying grains in rocks with weak remanence. Comparisons between AIRM and other measures of magnetic fabric allow for description of mineral-specific or grain-size-dependent fabrics, and their relation to one another. Additionally, when the natural remanence of a rock is carried by high-coercivity minerals, it is essential to isolate the anisotropy of this grain fraction to correct paleodirectional and paleointensity data. AIRMs have been measured using a wide range of applied fields, from a few mT to several T. It has been shown that the degree and shape of AIRM can vary with the strength of the applied field, for example, due to the contribution of separate grain subpopulations or due to field-dependent properties. To improve our understanding of these processes, we systematically investigate the variation of AIRM and the anisotropy of partial isothermal remanence (ApIRM) with applied field for a variety of rocks with different magnetic mineralogies. We also test the additivity of A(p)IRMs and provide a definition of their error limits. While A(p)IRM principal directions can be similar for a range of applied field strengths on the same specimen, the degree and shape of anisotropy often show systematic changes with the field over which the (p)IRM was applied. Also, the data uncertainty varies with field window; typically, larger windows lead to better-defined principal directions. Therefore, the choice of an appropriate field window is crucial for successful anisotropy corrections in paleomagnetic studies. Due to relatively large deviations between AIRMs calculated by tensor addition and directly measured AIRMs, we recommend that the desired A(p)IRM be measured directly for anisotropy corrections.

Key words: Magnetic properties; Magnetic fabrics and anisotropy; Rock and mineral magnetism.

1 INTRODUCTION

Magnetic fabrics are a fast and efficient measure of mineral textures (Owens 1974; Hrouda 1982; Rochette *et al.* 1992; Tarling and Hrouda 1993; Borradaile and Henry 1997; Martín-Hernández *et al.* 2004; Borradaile and Jackson 2010). Anisotropy of remanent magnetization, in particular, provides information on the preferred alignment of remanence-carrying grains, and can be used to correct paleodirectional and paleointensity data for the effects of anisotropic remanence acquisition (Stephenson *et al.* 1986; Jackson 1991; Jackson and Tauxe 1991; Biedermann *et al.* 2019a). The anisotropy of anhysteretic remanent magnetization (AARM) is often chosen for these purposes because it is considered the best room-temperature equivalent of a natural thermoremanent magnetization (Potter 2004). However, AARM measurements target lowand intermediate-coercivity grains and are thus mainly applicable to

samples whose remanence is carried by magnetite and its titaniumsubstituted equivalents. By contrast, the anisotropy of isothermal remanent magnetization (AIRM) targets also the high-coercivity remanence carriers that are not magnetized in the weak fields used during AARM measurements (Cox and Doell 1967). For this reason, AIRM is preferentially used to correct paleomagnetic data in hematite-rich sediments or lunar rocks (Stokking and Tauxe 1990; Hodych and Buchan 1994; Font et al. 2005; Tamaki and Itoh 2008; Bilardello and Kodama 2009; Tikoo et al. 2012; McCall and Kodama 2014; Garrick-Bethell et al. 2016). An additional advantage of AIRM is that isothermal remanences (IRMs) are stronger than anhysteretic remanences (ARMs). Therefore, IRMs imposed in low fields (e.g. $\leq 60 \,\mathrm{mT}$) have been used to characterize the magnetite contribution to remanence anisotropy (Stephenson et al. 1986; Tarling and Hrouda 1993; Bogue et al. 1995; Cagnoli and Tarling 1997; Bascou et al. 2002; Raposo et al. 2003; Kovacheva et al. 2009; di

Capua 2014). A survey of earlier AIRM research has shown that depending on the goal of a study, the anisotropy of IRM can be measured by applying fields between a few mT and 13 T in a number of specimen orientations (typically 3 or 9), or by measuring IRM acquisition curves along several directions. Most studies used pulse magnetizers to impart IRMs. Sometimes, specimens were demagnetized between magnetizing steps in different directions; however, this was not always possible, especially when the IRM fields were greater than the maximum demagnetizing alternating fields (AFs) available. If a specimen saturates in the applied field, then demagnetization between directions is not necessary. Another approach to avoid problems of residual magnetization is using multiple specimens to define the anisotropy, which also avoids issues of thermochemical alteration (Bilardello 2015). In summary, AIRM is preferred over AARM mainly in two cases: (1) when rocks are dominated by high-coercivity remanence carriers (Kodama and Dekkers 2004), or (2) when a rock's remanence is near the sensitivity of one's rock magnetometers (Potter 2004).

As a consequence of the different minerals it targets, when combined with other methods, AIRM can provide additional information on the nature of magnetic and mineral fabrics that could not be obtained from one method alone. For example, Lu and McCabe (1993) compared AARM and AIRM in carbonate rocks from the Nashville (Tennessee, USA) and the Jessamine (Kentucky, USA) domes, and found that their AARM reflects both a depositional and compaction fabric, while the AIRM represents a later tectonic overprint. Henry and Daly (1983) and Hrouda (2002b) proposed that paramagnetic and ferromagnetic contributions to the magnetic fabrics can be separated based on a comparison between anisotropy of magnetic susceptibility (AMS) and AIRM (but see caveats in Hrouda et al. 2000). More recent separation methods exploit the different fieldand temperature-dependencies of paramagnetic and ferromagnetic properties (Martín-Hernández and Ferré 2007). Numerous studies have used combinations of AMS, AARM, AIRM and anisotropy of thermal remanence (ATRM) to better understand the carriers of magnetic fabrics, in aid of their interpretation (Borradaile and Dehls 1993; Selkin et al. 2000; Lawrence et al. 2002; Raposo et al. 2004; Tema 2009; Bilardello and Jackson 2014; Biedermann et al. 2016; Agro et al. 2017; Lycka 2017).

While a comparison between AMS, AARM, ATRM and AIRM is useful for a first characterization of different carrier minerals and their fabrics, it is possible to separate different grain subpopulations even more deliberately. Subpopulations of remanencecarrying grains may define distinct fabrics for different grain sizes or compositions, resulting, for example, in AARMs and anisotropy of partial ARMs (ApARMs) that vary with coercivity (Jackson et al. 1989; Trindade et al. 2001; Aubourg and Robion 2002; Usui et al. 2006; Biedermann et al. 2019a,b). A recent study illustrates how these coercivity-dependent variations of remanence anisotropy may cause problems for the interpretation of paleodirectional and paleointensity data, and how ApARM-based anisotropy corrections can be improved (Biedermann et al. 2019a). Similarly, AIRMs can vary with applied field, which may be attributed to anisotropy components carried by different subpopulations of grains. For example, several generations of hematite were found in hematite-bearing Cambrian slates from North Wales, where fine-grained hematite displays stronger fabrics than coarse-grained hematite (Jackson and Borradaile 1991). Bilardello (2015) used AIRMs determined in different fields to isolate the fabrics of pigmentary and detrital hematite, and also discusses issues related to incomplete saturation of hematite. Alternatively, field-dependent AIRMs in pyrrhotite

samples have been explained by competing texture- and grain-size-control of the anisotropy (de Wall and Worm 1993). Tensor subtraction of the AIRM measured in several fields has been used to calculate the ApIRM of certain coercivity windows (Bogue *et al.* 1995). Additionally, AIRMs can be partially demagnetized by thermal or AF methods to isolate only the high unblocking temperature or high-coercivity (e.g. hematite) parts of the remanence fabric (Cox and Doell 1967; Tan and Kodama 2002; Tan *et al.* 2003; Kodama and Dekkers 2004; Bilardello and Kodama 2009; Hillhouse 2010; Bilardello 2015; Biedermann *et al.* 2016).

Because magnetization M saturates in high fields, high-field IRM is not a linear function of the applied field H or B. Therefore, it is important to consider how high-field anisotropy is mathematically described. Second-order tensor mathematics, assuming a linear dependence of M upon H (Jelinek 1977), are often used to characterize IRM anisotropy. This is done with the implicit understanding that while this is not strictly correct (Coe 1966), it remains a useful approximation. Similarly, the low-field susceptibilities of hematite, pyrrhotite and titanomagnetite are field dependent over the range of AC fields typically used, up to a few hundred A m⁻¹ (H) or μ T (B) (Worm 1991; de Wall and Worm 1993; Jackson et al. 1998; de Wall 2000; Hrouda 2002a; Guerrero-Suarez and Martin-Hernandez 2012). For these minerals, the magnetic fabric tensors calculated from linear AMS theory may represent an inaccurate description of anisotropy. In some instances, the linear fit to nonlinear data may result in erroneous negative minimum susceptibilities (Hrouda 2002a). Possible ways to account for the nonlinearity of magnetization with field in these minerals are (1) measuring in extremely low fields, $< 10 \text{ A m}^{-1}$, where the M(H) behaviour is still linear, (2) measuring many additional orientations and describing the anisotropy using a higher order tensor or (3) using the Rayleigh law to compute initial susceptibilities in each orientation, for which tensor calculations are valid (Hrouda 2002a; Hrouda 2009; Hrouda et al. 2018). These methods have their own limitations in terms of sensitivity, precision and efficiency. Although the degree of anisotropy can vary strongly with field, principal directions and anisotropy shape, the main parameters used for geologic interpretations show a weaker field dependence (de Wall 2000; Hrouda 2002a; Hrouda 2009). Hrouda et al. (2018) have compared AMS tensors calculated using linear theory with contour plots from 320 directional susceptibility measurements in various fields for more than 100 specimens, and concluded that the second-order tensor describes the specimens' anisotropy to sufficient accuracy. For high-field IRMs and AIRMs, the departure from linearity may be much larger than for the lowfield induced magnetization and low-field AMS, and the effects of treating them with tensor mathematics require further study.

Here, we investigate whether and how the A(p)IRM varies with coercivity window in different rock types. In addition, we test whether ApIRMs are additive and define error limits for this additivity. The results presented here improve our understanding of IRM anisotropy, and it is our hope that A(p)IRMs become more useful for studies involving magnetic fabrics and anisotropy.

2 MATERIALS AND METHODS

2.1 Sample collection

The sample collection used for this study includes five specimens from the Bushveld Complex, South Africa (label prefix BG), one specimen from the Bjerkreim Sokndal layered intrusion, Southern Norway (BK), two ocean floor gabbros (ODP735), three metamorphic slates from the Thomson Formation (TS) and five red bed sediment specimens from the Mauch Chunk Formation (MC). The Bushveld samples contain micrometer-sized Ti-magnetite needles and hematite platelets, exsolved within pyroxene and plagioclase. The rocks from Bjerkreim Sokndal contain hemo-ilmenite, either exsolved in pyroxenes or as individual grains, and magnetite. Oceanic gabbros from ODP hole 735B contain both primary Timagnetite, and secondary magnetite as exsolutions or formed by alteration of pyroxene and olivine, as well as sulfides. The slates from the Thomson Formation contain magnetite and possibly sulfides, and the red bed sediments contain trace amounts of magnetite, and both detrital and pigmentary hematite. The magnetic mineralogy and anisotropy of susceptibility and ARM of these specimens have been described previously (Johns et al. 1992; Pariso and Johnson 1993; Sun et al. 1995; McEnroe et al. 2001; Tan and Kodama 2002; Feinberg et al. 2006; Bilardello and Kodama 2010; Biedermann et al. 2016, 2019b,c).

2.2 Initial test measurements

For robust anisotropy characterization, it is essential that the directional differences among acquired magnetizations are larger than the variability of repeated measurements along the same direction. Therefore, test measurements were conducted prior to AIRM determination to check the repeatability of an IRM imparted in a 100 mT field along the specimens' axes. All magnetizations were measured on a 2G 760 superconducting rock magnetometer (SRM). Magnetization tests were performed using a pulse magnetizer (2G, long core) or a vibrating sample magnetometer (VSM, Princeton Model 3900). For the latter, pick-up coils were removed to obtain a better geometry to fit a sample holder for directional IRMs, maximize the applied field strength and protect the pick-up coils themselves. Imparting IRMs on a pulse magnetizer is faster, but has the disadvantage that other instruments have to be used to demagnetize the specimens: an AF demagnetizer in low fields, and the electromagnets of a VSM in high fields. The VSM can reach higher fields, but uses a lower frequency than conventional AF units; 10-100 s of field cycles as compared to 1000-10000 s of field cycles. Concerns have been raised about the accuracy and reproducibility of fields produced by the pulse magnetizer, in particular related to backfield generation at high fields. For example, it has been recommended to use at least two pulses to magnetize u-channel samples (Roberts 2006). Magnetizing specimens on the VSM takes longer, but offers the advantages of better field control, and that specimens can be demagnetized directly on the VSM in fields equal to or slightly above those in which the IRMs were imparted. In this study, repeat measurements of IRMs imparted parallel to x, y and z were used for the pulse magnetizer, and IRMs along x and y were used for the VSM. For the pulse magnetizer, these test measurements show that (1) the variability of IRMs parallel to any axis is rather large compared to the differences between axes, and (2) the magnetization acquired parallel to the previous axis is not fully remagnetized when the magnetization along the next axis is applied (Fig. 1a). This second issue is minimized when demagnetization steps are included between pulse magnetization steps. Similar measurements on the VSM show a smaller variation between repeat measurements (Fig. 1b).

Applying progressively higher IRMs up to 1 T along the specimen *x*-axis reveals an additional difficulty: using the standard mode to

turn the field on and off leads to overshooting, that is, the application of a backfield recoil, resulting in lower IRMs at higher fields. This can be explained by the fact that when applying a higher field, the backfield generated during switch-off of the field is larger. A lower field pulse, but equal or higher to that of the recoil must be subsequently applied to obviate this effect. The VSM possesses a non-overshoot mode for toggling the field, and this results in IRMs that increase monotonically with applied field and reach saturation, as expected (Fig. 1c). Hence, all anisotropy measurements were conducted on the VSM, while toggling the field using the non-overshoot mode.

2.3 IRM acquisition

IRM acquisition was characterized on representative samples from each group, selected based on previous A(p)ARM measurements. It was measured following the double IRM acquisition method (Tauxe et al. 1990). This involves applying a field parallel to the specimen +z-axis and measuring the resulting IRM, followed by the same field along the -z-axis, on an initially demagnetized specimen. Based on the results from test measurements, the IRMs were applied on a VSM, and the non-overshoot function was used when turning the fields on and off. Specimens were demagnetized using the VSM's AF demagnetization at 1 T (1 per cent decrement), followed by a second demagnetization at 100 mT (1 per cent decrement). Acquisition fields were progressively increased from 0 to 5, 10, 20, 35, 50, 75, 100, 130, 180, 240, 320, 410, 500, 630, 800 mT and 1 T. The last field, 1 T along -z, was repeated three times to check repeatability. Magnetizations were measured on the 2G-760 SRM, and are reported as x-, y- and z-components, as well as IRM intensity. We will refer to the magnetizations imparted along +z as IRM acquisition, and those along -z as backfield curves.

The coercivity distributions derived from the IRM acquisition curves were analysed using the MAX Unmix software package (Maxbauer *et al.* 2016), to separate components of the coercivity distribution, and determine whether the coercivity spectra contain one or more distinct components. The IRM acquisition curves were not originally collected for coercivity unmixing and contain fewer data points per specimen than is typically recommended. As a result, the precise details of the fitted components should be viewed with a level of caution (e.g. skewness, dispersion and per cent contribution). However, statistical determinations of whether a data set is best fit by one or more components should remain robust. Unsmoothed spectra were used for all specimens except TS16.2 whose acquired IRM was the weakest, thus subject to a higher noise level.

2.4 Anisotropy of full and partial IRMs

A set of nine (p)IRM anisotropy tensors was determined for each specimen. Each tensor was based on IRMs imparted along nine directions in a specified field, and partial AF demagnetization of these remanences. The directions used were 0/0 (declination/inclination in specimen coordinates), 90/0, 0/90, 45/0, 135/0, 0/45, 90/45, 180/45, 270/45, following the schemes of McCabe *et al.* (1985) and Girdler (1961) for AARM and AMS, respectively. Directional IRMs were acquired on the VSM in fields of 100, 180, 500 mT and 1 T. After measuring the full IRM on the 2G-760 SRM, these IRMs were partially demagnetized at 100 and 180 mT on a DTech AF demagnetizer and the remaining pIRMs were measured. The fields of 100 and 180 mT were chosen because A(p)ARMs have previously been measured in the same fields (Biedermann *et al.* 2019b,c). Note that

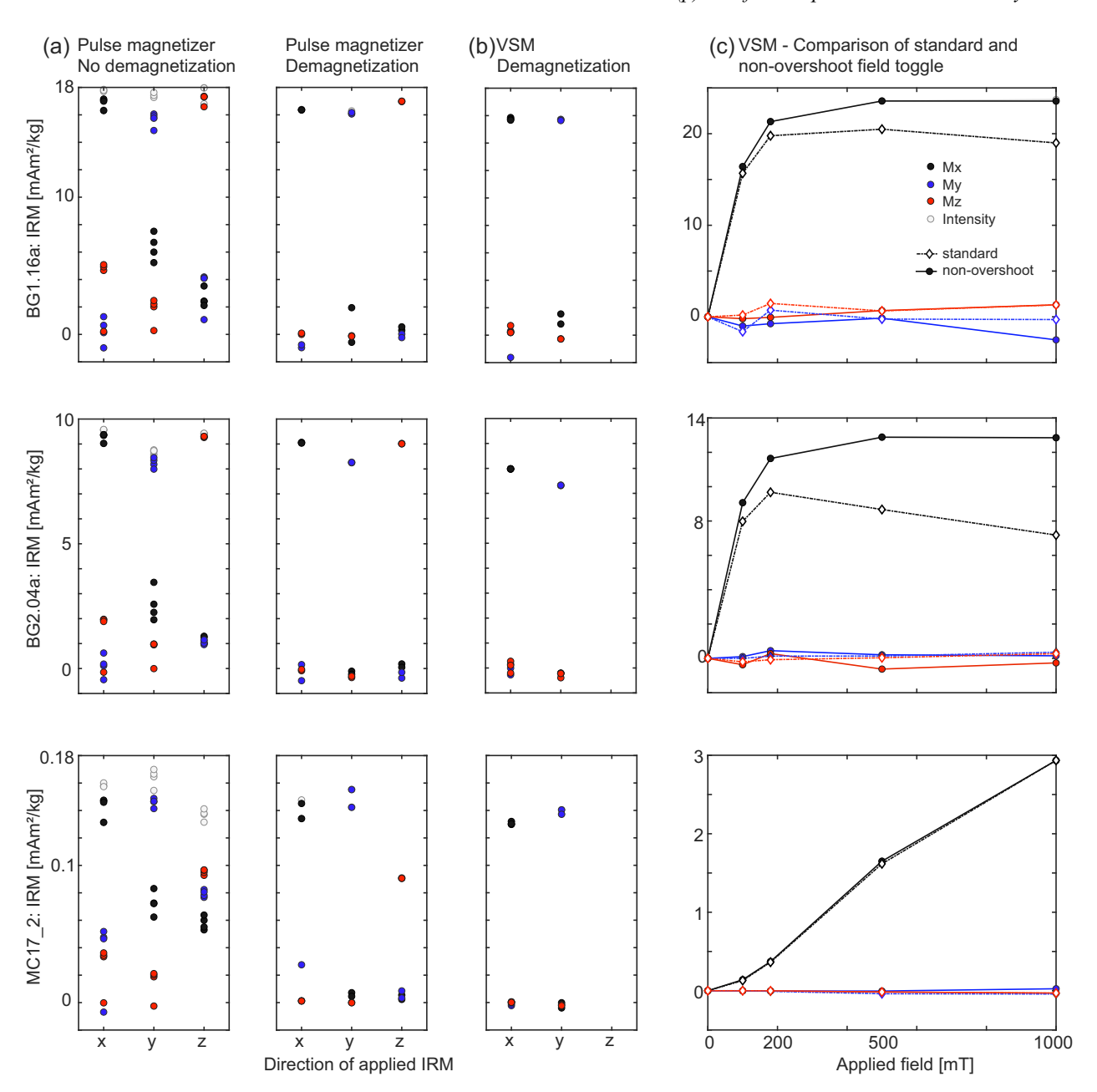


Figure 1. (a) Repeat IRM measurements parallel to the *x*, *y* and *z*-axes using a pulse magnetizer, with and without AF demagnetization in between steps. (b) Repeat IRM measurements parallel to *x* and *y* on the VSM. (c) Comparison of standard and non-overshoot modes of the VSM for IRMs applied parallel to *x*.

we are using the term 'full IRM' for magnetizations acquired prior to any partial demagnetization, even if a sample's magnetization does not fully saturate in the fields applied ($B_{\rm app}$). The term 'partial IRM' will be used for magnetizations that have been imparted in a field $B_{\rm app}$ and then AF demagnetized at 100 or 180 mT, that is, magnetized over the coercivity windows 100 to $B_{\rm app}$ mT, or 180 to $B_{\rm app}$ mT. Subsequent to imparting and measuring all IRMs and pIRMs along one direction, the specimens were AF-demagnetized on the VSM at 1 T followed by 100 mT, using 1 per cent decrements, as for the IRM acquisition experiments. The residual magnetization that could not be demagnetized between +1 and -1 T was subtracted from all directional IRMs as background. AIRM and ApIRM tensors were computed from the parallel components, that is, the magnetization acquired parallel to the applied field, of each directional magnetization. Thus, each specimen is characterized by

four AIRMs (AIRM $_{0-100}$, AIRM $_{0-180}$, AIRM $_{0-500}$ and AIRM $_{0-1000}$) and five ApIRMs (ApIRM $_{100-180}$, ApIRM $_{100-500}$, ApIRM $_{180-500}$, ApIRM $_{100-1000 \, \mathrm{and}}$ ApIRM $_{180-1000}$). Principal directions, degree and shape of the anisotropy were computed for each A(p)IRM tensor, and compared to one another. The principal directions correspond to the eigenvectors of the magnetization tensor, and the corresponding eigenvalues describe the maximum, intermediate and minimum principal magnetizations ($M_{\mathrm{max}} \geq M_{\mathrm{int}} \geq M_{\mathrm{min}}$). The degree of anisotropy is characterized by two parameters, $P = \frac{M_{\mathrm{max}}}{M_{\mathrm{min}}}$ and $M' = \frac{M_{\mathrm{min}}}{M_{\mathrm{min}}}$

 $\sqrt{((M_{\rm max}-M_{\rm mean})^2+(M_{\rm int}-M_{\rm mean})^2+(M_{\rm min}-M_{\rm mean})^2)/3}$ with $M_{\rm mean}=(M_{\rm max}+M_{\rm int}+M_{\rm min})/3$, analogously to P and k', respectively, for susceptibility anisotropy. Note that because IRMs saturate in strong fields, we prefer to use magnetizations rather than susceptibilities to define anisotropy parameters. The anisotropy shape is

described by $U=(2*M_{\rm int}-M_{\rm max}-M_{\rm min})/(M_{\rm max}-M_{\rm min})$ (Jelinek 1981; Jelinek 1984). For the purpose of this study, results are shown in specimen coordinates. Hext (1963)'s statistics was used to determine whether the presence of anisotropy and the directions of principal axes are statistically significant (if F<9.01 or $e_{13}>26^\circ$, anisotropy is not significant). For subsequent analyses (e.g. tensor addition), statistically insignificant tensors were replaced by an isotropic tensor with diagonal elements equal to $M_{\rm mean}$. The orientations of principal axes are at least partially undefined if $e_{12}>26^\circ$ or $e_{23}>26^\circ$.

2.5 Additivity of ApIRMs

If A(p)IRMs are additive, future studies could determine a small number of tensors and then compute additional tensors. To test whether AIRMs are additive, full AIRM tensors for fields $\geq\!180\,\text{mT}$ were computed from sets of measured AIRMs and ApIRMs, and compared to the measured tensors in the same field. Tensors were calculated as follows:

$$AIRM_{0-180,c} = AIRM_{0-100} + ApIRM_{100-180}$$

$$AIRM_{0-500,c1} = AIRM_{0-100} + ApIRM_{100-500}$$

$$AIRM_{0-500,c2} = AIRM_{0-180} + ApIRM_{180-500}$$

$$AIRM_{0-500,c3} = AIRM_{0-100} + ApIRM_{100-180} + ApIRM_{180-500}$$

$$AIRM_{0-1000,c1} = AIRM_{0-100} + ApIRM_{100-1000}$$

$$AIRM_{0-1000,c2} = AIRM_{0-180} + ApIRM_{180-1000}$$

$$\begin{split} AIRM_{0-1000,c3} &= AIRM_{0-100} + ApIRM_{100-180} \\ &+ ApIRM_{180-1000}. \end{split}$$

The group of calculations AIRM....c1 will be called $0-100-B_{\rm app}$, AIRM....c2 are referred to as $0-180-B_{\rm app}$ and AIRM....c3 as $0-100-180-B_{\rm app}$. Additivity was evaluated in terms of the agreement between mean IRMs, directions of principal axes, anisotropy degree and shape parameter, as well as tensor elements, for the sum of ApIRM and the corresponding measured AIRM tensors. The agreement between summed and directly measured tensors was quantified by the ratios of calculated and measured values for mean remanence and anisotropy degree, differences for the shape parameter and angular differences relative to the confidence angles for principal directions, analogously to the assessment of A(p)ARM additivity described in Biedermann *et al.* (2019c).

3 RESULTS

3.1 IRM acquisition and coercivity spectra

Most specimens show a strong initial increase in IRM up to DC fields of 200–300 mT, followed by a weaker increase at higher fields

(Fig. 2). Specimen MC17_2, a red bed sediment from the Mauch Chunk formation, does not acquire any IRM in fields <10 mT, followed by a gradual increase. This specimen does not saturate in a 1T field, the maximum that could be reached with the pole configuration used on the VSM, and prior work has shown that 4.75 T is necessary to saturate hematite's remanence within and perpendicular to bedding (Bilardello 2015). In the same specimen, backfield IRMs are significantly weaker than the IRMs acquired in the same field, which may be due to hematite's multiaxial basalplane anisotropy (Mitra et al. 2011; Mitra et al. 2012). Similarly, the Thomson Formation slates do not saturate completely in a 1 T field. Unmixing of the coercivity spectra favours two-component models over single components, as indicated by the F-test at 95 per cent confidence (Supporting Information Table A). Additional components at higher fields cannot be excluded. Note that for all specimens, while the IRMs were imparted parallel to the specimens' z-axes, the magnetizations acquired also possess components along the specimen x- and y-axes, which is a direct consequence of remanence anisotropy. Repeat application of an IRM in the same direction leads to a 1.2-2.5 per cent increase in magnetization for specimens MC17_2 and TS16.2 that do not saturate in a 1 T field, and 0.06-0.7 per cent change in the remaining specimens. A similar kind of progressive increase in repeated IRM has been observed in treatments of u-channel samples, but attributed to artefacts of the pulse magnetizer (Roberts 2006). Because we observe changes in IRM acquired on the VSM, and as they are strongest for non-saturated specimens, we argue that small changes occur in magnetization that seem likely to be time-dependent effects but remain to be fully analysed.

3.2 AIRMs and ApIRMs

Nine tensors each were measured on 16 specimens. The full directional IRMs in one specimen, ODP735.042, were so strong that they could not be measured reliably, so that for this specimen, only the five ApIRM tensors are reported. The mean (p)IRMs of specimens that could be measured vary over several orders of magnitude, from 3.47×10^{-7} to $2.50 \times 10^{-2} \,\mathrm{Am^2\,kg^{-1}}$ (Supporting Information Table B). A total of 140 A(p)IRM tensors have been characterized, and 28 of these do not possess statistically significant anisotropy. It is mainly the low-coercivity AIRMs and ApIRMs of the Mauch Chunk red bed samples, and the high-coercivity ApIRMs of the Thomson Slate and ocean floor gabbro that are not significant. A likely explanation for this is that only weak (p)IRMs are acquired by these sample groups in the respective coercivity windows, thus leading to a higher influence of noise on the anisotropy tensor calculation. The lack of IRM acquisition in low fields or low-field IRM anisotropy in some red bed samples is related to negligible amounts of magnetite, or no magnetite anisotropy, respectively. In contrast, the Thomson Slate and ocean floor gabbro specimens contain predominantly low-coercivity minerals such as magnetite and titanomagnetite, so that the mean high-field pIRMs are weak.

For those specimens that do have significant anisotropy, P varies between 1.06 and 4.79. The highest P-values are observed for low-coercivity AIRMs of those Mauch Chunk red bed specimens that seem to display significant anisotropy. It has been shown previously that noise on a weak susceptibility signal can lead to unrealistically high P-values as well as a large spread in shape parameters for AMS measurements (Hrouda 1986; Hrouda 2004; Biedermann $et\ al.\ 2013$). A similar effect may explain the seemingly high P-values of the AIRM $_{0-100}$, AIRM $_{0-180}$ and ApIRM $_{100-180}$ in these

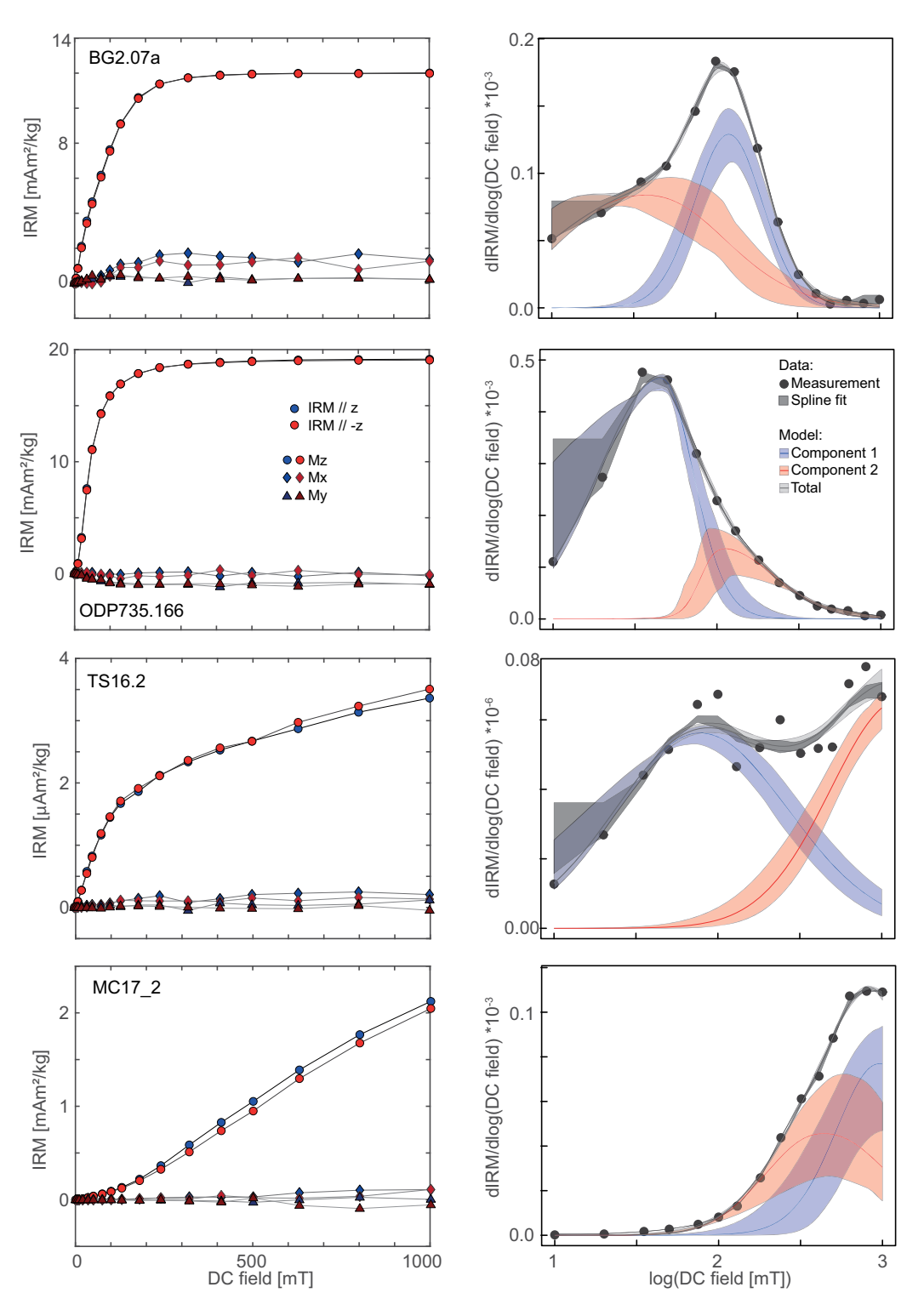


Figure 2. Left-hand column: IRM acquisition and backfield curves for selected specimens. The magnetization was applied parallel to +z (acquisition) and -z (backfield); right-hand column: coercivity distribution and unmixing of magnetic components. The contribution of each component as well as their total coercivity spectra is shown as median distributions with 95 per cent confidence limits.

red beds. The parameter M' varies between 7.62×10^{-8} and 1.16×10^{-3} Am 2 kg $^{-1}$, which corresponds to 2.3–53 per cent of the mean (p)IRM obtained by the respective specimens in the respective windows. The anisotropy shape U covers the range from -0.79 to 0.84.

Principal directions, degree and shape of the anisotropy can be similar or vary between different ApIRMs and AIRMs in the same specimen. The principal directions in the Bushveld specimens can have similar orientations, or show two or three distinct sets of directions. In the latter case, the main difference is often between the AIRMs and the ApIRMs, where different coercivity subpopulations may be associated with subsets of exsolved oxide inclusions in silicate minerals such as plagioclase and pyroxene. The Bjerkreim

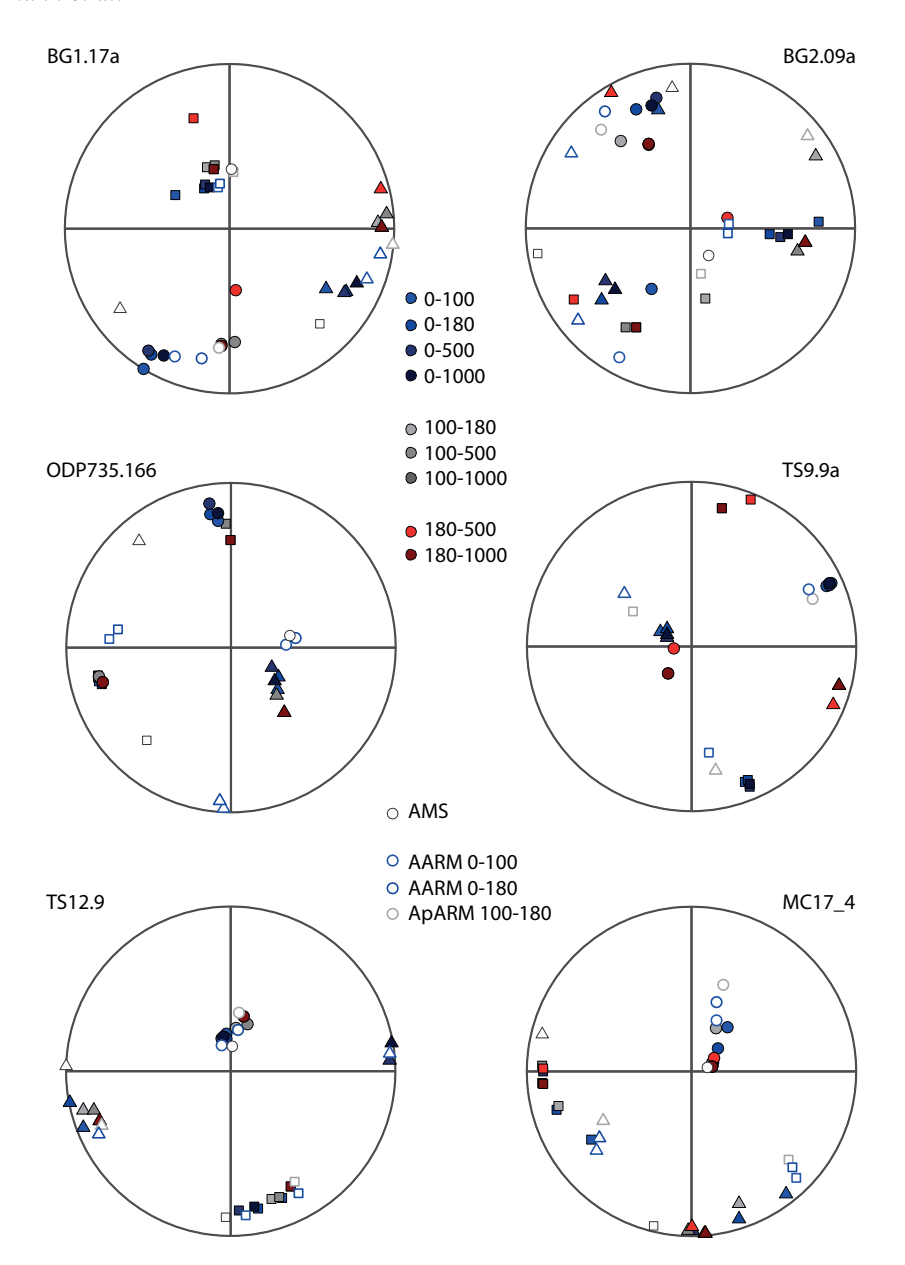


Figure 3. Principal directions of the AIRM and ApIRM tensors for a selection of representative specimens. The squares, the triangles and the circles represent the maximum, intermediate and minimum magnetization directions, respectively, and colours refer to the windows over which the (p)IRMs were imposed. The open symbols are the corresponding AARM, ApARM and AMS fabrics reported by Biedermann *et al.* (2019b).

Sokndal specimen has similar orientations for all A(p)IRM tensors. The one ODP735 gabbro for which all tensors could be measured, exhibits a switch of maximum and minimum principal directions between AIRM and ApIRM tensors. Two Thomson Slate specimens show similar orientations of all A(p)IRMs, and the third one has different principal directions in the ApIRM_{180-Bapp} windows as opposed to the AIRM and the ApIRM_{100-Bapp} where significant. For the Mauch Chunk red beds, four specimens display similar orientation for all A(p)IRMs that are significant, and one specimen shows a similar orientation of the minimum axis, and a girdle distribution of the other two axes (Fig. 3).

For most specimens, M' is highest for the AIRMs followed by the ApIRM_{100-Bapp} and ApIRM_{180-Bapp}. The one exception to this general trend is the Mauch Chunk red bed sample suite, where the tensors incorporating the highest coercivities, that is, AIRM₀₋₁₀₀₀, ApIRM₁₀₀₋₁₀₀₀ and ApIRM₁₈₀₋₁₀₀₀, have the strongest anisotropies.

The anisotropy parameters M', P and U vary with the field in which the (p)IRM was acquired, and these variations appear consistent between different specimens from the same locality (Fig. 4).

3.3 Additivity

The calculated mean IRM, obtained by summing the appropriate (p)IRM tensors, is generally lower than the corresponding measured mean IRM. For calculations involving the tensors $0-100-B_{\rm app}$ and $0-100-180-B_{\rm app}$ (AIRM $_{0-180,c}$, AIRM $_{0-500,c1}$, AIRM $_{0-500,c3}$, AIRM $_{0-1000,c1}$, AIRM $_{0-1000,c3}$), the ratio of calculated to measured mean IRM can be as low as 0.9. Calculations $0-180-B_{\rm app}$ (AIRM $_{0-500,c2}$, AIRM $_{0-1000,c2}$) are slightly more accurate, with the calculated mean being ≥ 0.95 times the measured mean. The calculated M' ranges from ca. 0.5 to ca. 1.5 times the measured M'. Similar to the mean IRM, the variation appears smaller for the

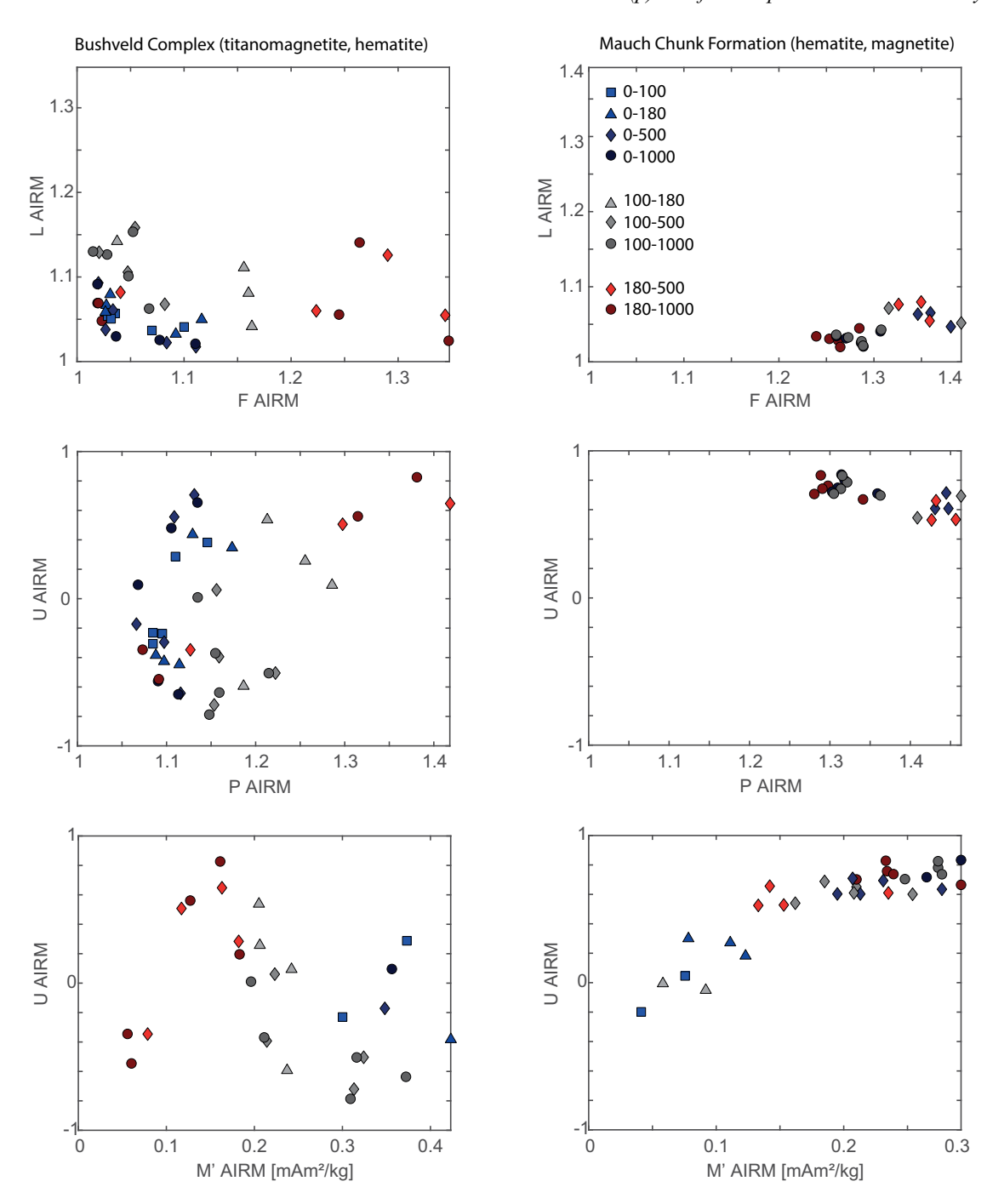


Figure 4. Anisotropy parameters of A(p)IRMs as a function of coercivity window for representative sample groups.

 $0{\text -}180{\text -}B_{\text{app}}$ calculations than those based on $0{\text -}100{\text -}B_{\text{app}}$ and $0{\text -}100{\text -}180{\text -}B_{\text{app}}$. The variations in shape parameters are about ± 0.5 (Fig. 5). Differences can be observed between the behaviours for each sample group. However, the number of specimens per group was small, so that this observation may be biased by the statistics of small numbers. Hence, they will not be interpreted further.

The angular deviations between the measured and calculated maximum and minimum principal directions are generally smaller than the 95 per cent confidence angles of the measurements for the Mauch Chunk, Thomson slate and ODP735 ocean floor gabbro specimens. The angle between measured and calculated maximum principal directions was compared to the e_{12} confidence angle, and

that between the minimum principal directions to e_{23} of the measured AIRMs. Because the deviation between measured and calculated directions is smaller than the confidence angles, the calculated and measured principal directions cannot be statistically distinguished on the 95 per cent confidence level. For most Bushveld specimens and the Bjerkreim Sokndal specimen, however, the angle between calculation and measurement is larger than the confidence angle for at least one of these axes, meaning that the principal directions calculated by tensor addition are significantly different from those measured. In accordance with the other parameters, the difference between measured and calculated principal directions is smallest for the 0–180- $B_{\rm app}$ calculations.

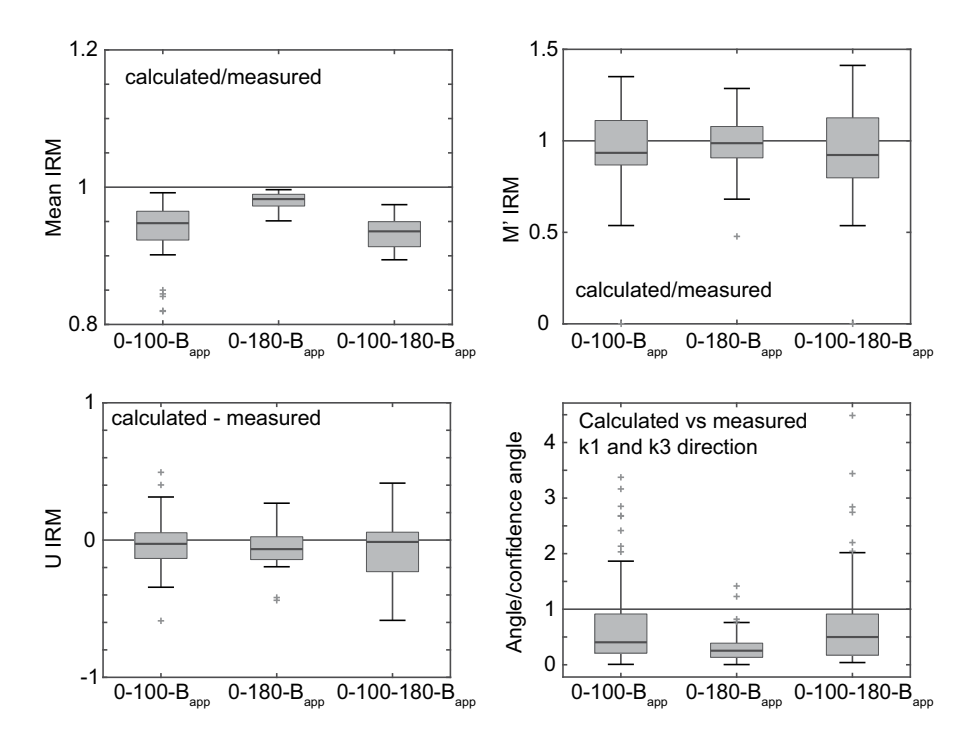


Figure 5. Comparison of calculated anisotropy parameters to measured anisotropy parameters. The black line indicates median, box contains the data from the 25th to 75th percentile, and whiskers extend to the last data point within 1.5 times the interquartile range. The latter corresponds to 99 per cent of the data points as long as data are normally distributed. The crosses show data points considered as outliers.

4 DISCUSSION

4.1 Variation of A(p)IRM with DC field

Similar to the coercivity dependence of ARM anisotropy (Jackson et al. 1988; Jackson et al. 1989; Biedermann et al. 2019a,b), IRM anisotropy varies with the strength of the DC field in which the remanence was acquired. The degree and shape of anisotropy are generally different within each field window. In samples from the Bushveld Complex, the shape parameter U varies between -0.8and +0.8, and the degree of anisotropy, M', covers the range from 0 to $1.2 \times 10^{-3} \,\mathrm{Am^2\,kg^{-1}}$, or 0–15 per cent of the mean (p)IRM. Different A(p)IRM subfabrics in the Bjerkreim Sokndal specimen cover shape values between 0.1 and 0.4, and M' between 0 and $5.1 \times 10^{-4} \,\mathrm{Am^2\,kg^{-1}}$, up to 12 per cent of the mean (p)IRM. The anisotropy tensors for the ODP735 specimens that could be measured possess U in the range of -0.6 to +0.3, and M' in the range of 0 to 1.1×10^{-3} Am² kg⁻¹, up to 8 per cent of the mean (p)IRM. Thomson slate specimens display U from -0.6 to +0.8, M' from 0 to $2.1 \times 10^{-6} \,\mathrm{Am^2\,kg^{-1}}$, up to 24 per cent of the mean remanence, and red bed specimens from the Mauch Chunk Formation have U between -0.2 and +0.8, and M' between 0 and $3.6 \times 10^{-4} \,\mathrm{Am^2 \, kg^{-1}}$ or up to 53 per cent of the mean (p)IRM in the respective windows. Although some uncertainty is associated with each measurement, measurement errors cannot explain the entire variation amongst tensors measured in different fields.

For lithologies where more than three specimens were measured, there are smaller variations between anisotropy parameters measured in each field window on all specimens from the site compared to those seen in the same specimen but for different windows (Fig. 6). Therefore, differences between anisotropy parameters measured in specific field windows can be interpreted as discrete subpopulations of grains—defined by their mineralogy, composition, grain size and shape—having distinct fabrics. Bilardello (2015) had

investigated changes of anisotropy degree and shape with coercivity during a stepwise demagnetization of IRMs acquired in 1 and 5.5 T fields on Mauch Chunk samples from the same location as those studied here. That study attributed changes in anisotropy parameters to (1) non-saturation of hematite in 1 T fields, and (2) differences in coercivity of specular versus pigmentary hematite and additional accessory magnetite. This study shows further examples of rocks whose IRM anisotropy varies with DC field, also when magnetite or iron sulfides dominate the anisotropy. Whether these results are directly relevant to other magnetic fabric investigations depends on the main focus of those studies, the mineral populations present and the fields needed to saturate their remanence. In any case, the results presented here lay a solid foundation for future work on the field dependence of IRM anisotropy.

Analogous to AMS and A(p)ARM, the highest anisotropy is not necessarily carried by the same grain fraction as the highest mean (p)IRM. The same specimen can display significant anisotropy in some coercivity windows, but not in others, and the ApIRMs carried by different subpopulations can add up or cancel each other out. Therefore, care needs to be taken when interpreting AIRMs in fabric studies because, similar to AMS or AARM, they can reflect composite fabrics. For the same reason, the field in which A(p)IRMs are measured needs to be chosen carefully when these tensors are used in paleomagnetic and paleointensity studies to correct for anisotropic remanence acquisition in high-coercivity grains. Isolating an appropriate anisotropy tensor prior to anisotropy corrections is crucial, as these corrections can have major implications for apparent polar wander paths (Bilardello and Kodama 2010). When the remanence is carried by a combination of subpopulations, paleomagnetic results are further affected by the differences in remanence anisotropy between carriers, which needs to be taken into account during anisotropy corrections (Biedermann et al. 2019a). Breaking down the full AIRM to individual ApIRMs can help determine how remanence anisotropy changes for each subpopulation

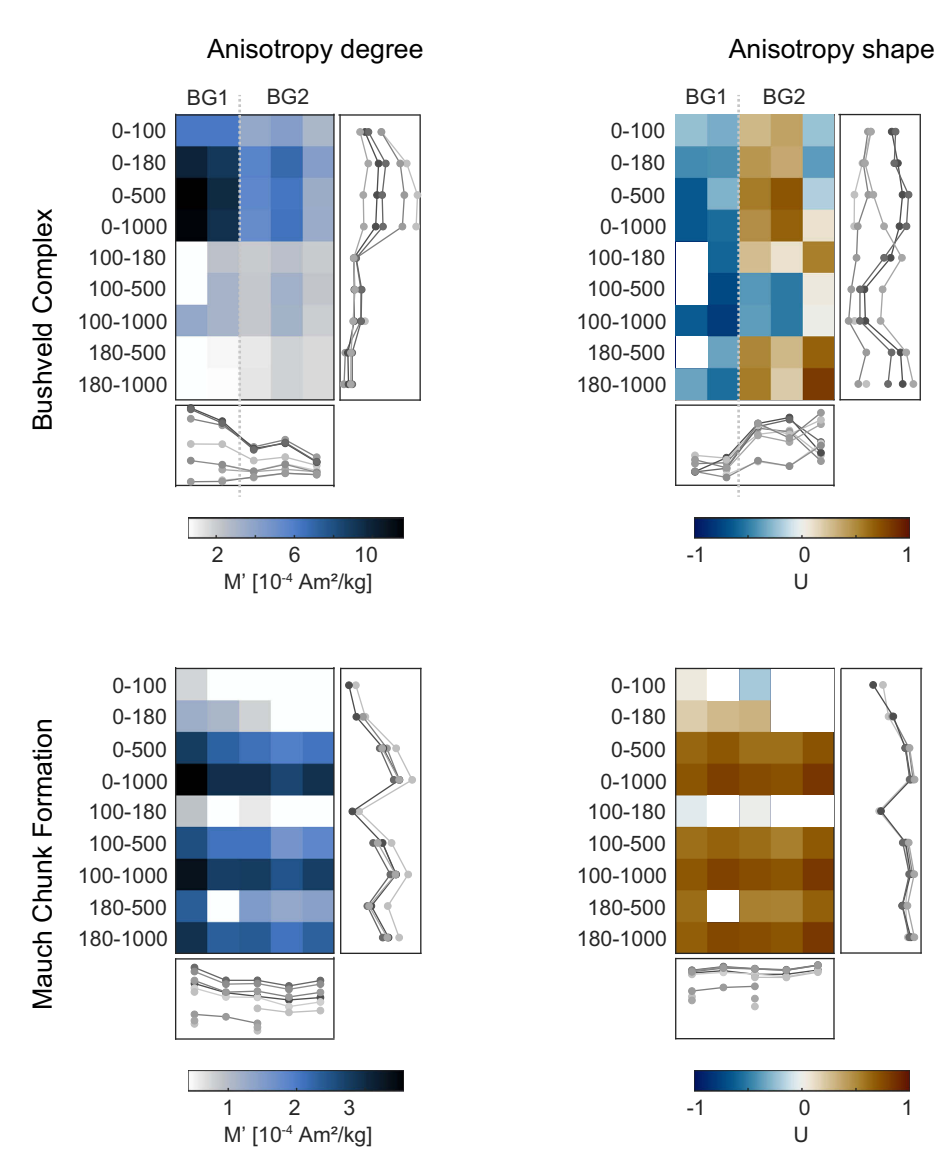


Figure 6. Anisotropy degree and shape of the Bushveld and Mauch Chunk samples. Variations with DC field compared to variations between different specimens and sites. White indicates fields and specimens whose anisotropy was not statistically significant. Perceptually uniform colour-maps are used to prevent visual distortion of the data (Crameri 2018).

in the specimen, and provides a solid basis for the reliable interpretation of both fabric and paleomagnetic data. A solid indication that a specimen possesses a composite IRM anisotropy is when the magnetization direction changes during an IRM acquisition or IRM demagnetization experiment. Note that the absence of changes in magnetization direction is not a reliable indicator for the absence of multiple contributors to AIRM, as the fabrics could be aligned but have different anisotropy degrees.

4.2 ApIRM additivity

Mean IRMs are underestimated when calculated from tensor addition of ApIRMs, especially when the added tensors contain the terms AIRM $_{0-100}$ + ApIRM $_{100\text{-}Bapp}$. In this study, errors can be as high as 10 per cent of the measured mean IRM. Smaller errors, \leq 5 per cent, are observed when adding AIRM $_{0-180}$ + ApIRM $_{180\text{-}Bapp}$. The latter error limit is of similar magnitude to that for mean ARM additivity (Yu *et al.* 2002; Biedermann *et al.* 2019c). One possible reason

for the variation of error with field is that the IRM varies strongly with field before specimens reach saturation at around 200–300 mT, but little variation of IRM with DC field is observed for higher fields, when the low-coercivity grains are saturated. Therefore, a small variability in DC field, when imparting the IRM, will have a larger effect on the acquired remanence at 100 mT than at higher fields. Analogously, if the AF demagnetizing field slightly deviates from the set field during a partial AF demagnetization, the effect will be larger at 100 than 180 mT. Because the calculated AIRMs are lower than those measured, the initially applied field may have been slightly too low, or the demagnetizing field too high, both attributable to instrumental precision. This hypothesis can be further investigated and resolved once instrumentation has been developed that produces reliable and repeatable IRM fields. More reliable and reproducible IRM fields would also be beneficial for double-IRM acquisition experiments (Tauxe et al. 1990), and would prevent researchers from having to use several pulses to impart IRMs (Roberts 2006). A second possibility is that slight misalignment of the samples when imparting directional pIRMs would lead to a smaller

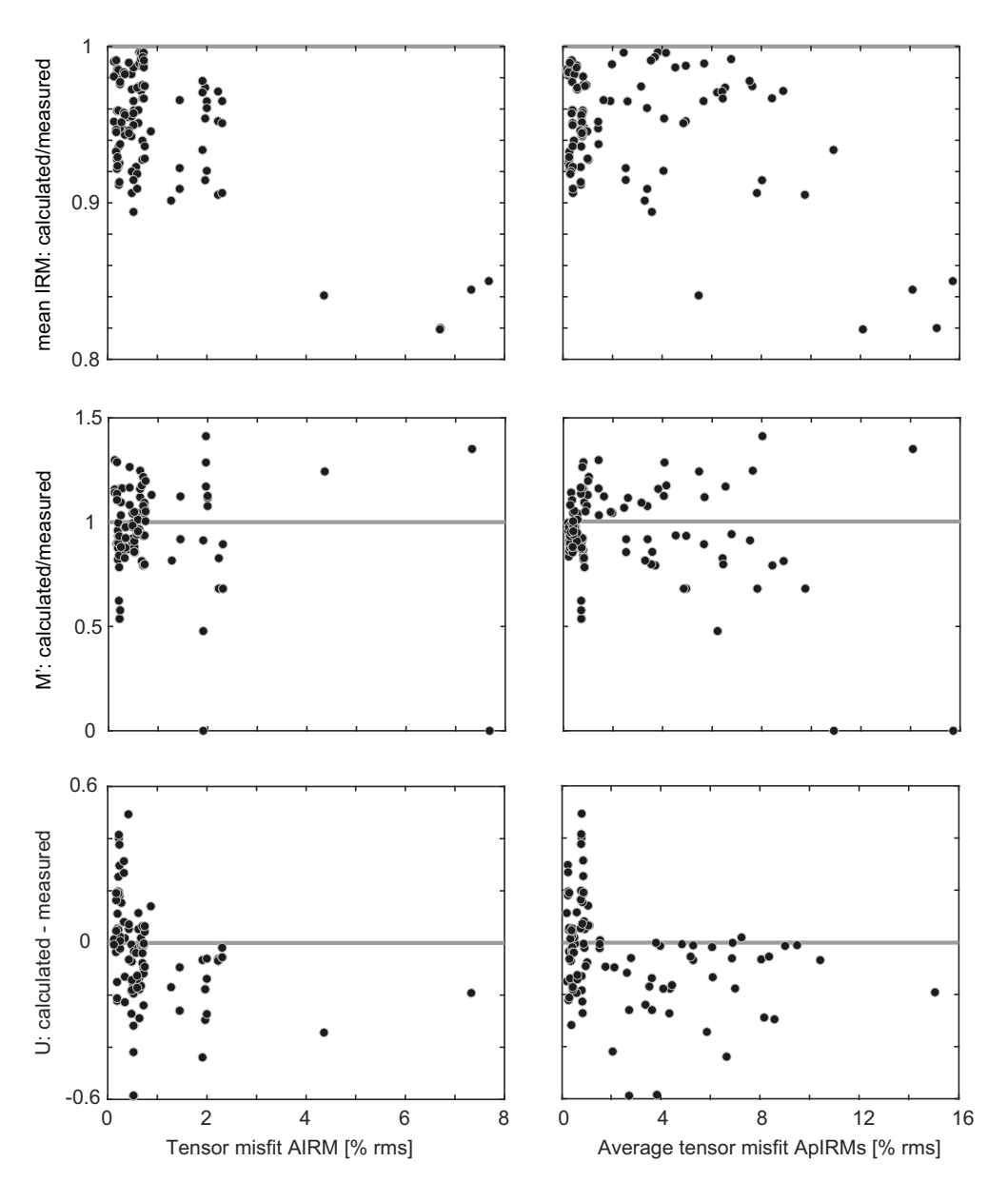


Figure 7. Deviations of measured and calculated AIRM parameters as a function of tensor misfit.

added directional IRM, and eventually a weaker added mean IRM compared to that measured. Although samples were carefully oriented in a specially designed holder for these measurements, small errors cannot be excluded completely. Another possible explanation for better additivity in the 0-180- $B_{\rm app}$ calculations, compared to 0-100- $B_{\rm app}$ and 0-100-180- $B_{\rm app}$, is that the pIRMs may not be fully independent: if this is the case, the effect on magnetization is larger at low fields where grains are not saturated than at high fields where they approach saturation or have saturated already. Further work needs to be conducted to investigate whether pIRMs are independent.

The main difference between AARM and AIRM measurements is that ARMs are usually weak enough to behave linearly with the field, whereas strong-field IRMs begin to approach saturation and thus are not linear with the applied field. Fitting a linear tensor equation to this nonlinear data may introduce errors, similar to and larger than those described for low-field AMS in field-dependent materials (Hrouda 2002a). It is possible that the larger uncertainty

in AIRM additivity stems from the nonlinearity of the directional IRMs with applied field. This would result in a correlation between tensor misfit (of either the ApIRM tensors used in the calculation, or the AIRM tensor the calculation is compared to) and the deviation of the calculated tensor from the measured tensor. The grouping of our data makes it hard to draw a general conclusion whether the uncertainty is related to tensor misfit. However, there appear to be larger deviations between calculated and measured mean IRMs when the tensor misfit is larger, and there is also more scatter for larger tensor misfits (Fig. 7). Similarly, larger scatter and larger deviations may be observed for other anisotropy parameters with increasing tensor misfit, but more data would be needed to make a general statement about the exact nature of such a correlation.

The error limits for principal directions and anisotropy parameters for A(p)IRM additivity are generally larger than the corresponding error limits determined for A(p)ARM on the same specimens (Biedermann *et al.* 2019c). Nevertheless, similar to A(p)ARM additivity, principal directions match best between measurement and

calculation, followed by degree of anisotropy and anisotropy shape. Therefore, when A(p)IRMs are to be used for anisotropy corrections, where all anisotropy parameters influence the final results and are thus important, we suggest that all necessary AIRMs and ApIRMs be measured directly, by imparting a set of directional IRMs followed by partial AF or thermal demagnetization, rather than derived from tensor addition and subtraction. In fabric studies with a main focus on the orientation of principal directions, rather than the exact values of P, M' and U, tensor calculations may be sufficient for a structural interpretation.

5 CONCLUSIONS

A total of 140 A(p)IRM tensors have been measured on 16 specimens from five geological settings. The samples were chosen to cover a range of remanence carriers and coercivity spectra. The results shown here illustrate that principal directions, degree and shape of AIRM and ApIRM depend on the coercivity window over which the remanence was imparted. This indicates that various subpopulations of grains together carry the remanence, and each of them possesses a distinct magnetic fabric. Hence, characterizing ApIRMs in addition to full AIRMs allows for more detailed tectonic and structural interpretations, and forms the basis for more advanced and accurate corrections of paleomagnetic data.

Tensor additions of A(p)IRMs generally underestimate the mean IRM compared to a direct AIRM measurement. The level of underestimation depends on whether individual ApIRM windows were chosen at low fields, before the specimen starts to approach saturation, or higher fields close to or above saturation. Error limits are larger in the former case. This may be related to small variability in the field generated to impart IRMs, which underscores the importance of developing more advanced instrumentation that can produce exact and repeatable fields. Another possibility that needs further work, is that pIRMs may not be fully independent. A third explanation, which will also need to be investigated further, is that the differences between measured and calculated parameters are related to the nonlinearity of isothermal magnetization with field. This nonlinearity means that second-order tensors are strictly not correct representations of the anisotropy, which results in misfits when calculating the tensor from the directional data.

For most specimens, calculated principal directions for summed pIRM tensors are within the 95 per cent confidence ellipses for the measured total AIRM. Error limits for anisotropy degree and shape can be as large as ± 50 per cent and ± 0.5 , respectively. Therefore, calculated AIRMs or ApIRMs may be suitable for fabric interpretations; however, we recommend measuring each tensor directly for paleomagnetic corrections.

ACKNOWLEDGEMENTS

Fatima Martin-Hernandez and Pedro Silva are thanked for their thoughtful and constructive reviews. This research was funded by the Swiss National Science Foundation, project 167608, and measurements were conducted at the IRM. The IRM is a US National Multi-user Facility supported through the Instrumentation and Facilities program of the National Science Foundation, Earth Sciences Division, and by funding from the University of Minnesota. Data are available in the Supporting Information. This is IRM publication 1811.

REFERENCES

- Agro, A., Zanella, E., Le Pennec, J.-L. & Temel, A., 2017. Complex remanent magnetization in the Kizilkaya ignimbrite (central Anatolia): implication for paleomagnetic directions, *J. Volc. Geotherm. Res.*, **336**, 68–80.
- Aubourg, C. & Robion, P., 2002. Composite ferromagnetic fabrics (magnetite, greigite) measured by AMS and partial AARM in weakly strained sandstones from western Makran, Iran, Geophys. J. Int., 151, 729–737.
- Bascou, J., Raposo, M.I.B., Vauchez, A. & Egydio-Silva, M., 2002. Titanohematite lattice-preferred orientation and magnetic anisotropy in high-temperature mylonites, *Earth planet. Sci. Lett.*, 198, 77–92.
- Biedermann, A.R., Lowrie, W. & Hirt, A.M., 2013. A method for improving the measurement of low-field magnetic susceptibility anisotropy in weak samples, J. Appl. Geophys., 88, 122–130.
- Biedermann, A.R., Heidelbach, F., Jackson, M., Bilardello, D. & McEnroe, S.A., 2016. Magnetic fabrics in the Bjerkreim Sokndal layered intrusion, Rogaland, southern Norway: mineral sources and geological significance, *Tectonophysics*, 688, 101–118.
- Biedermann, A.R., Bilardello, D., Jackson, M., Tauxe, L. & Feinberg, J.M., 2019a. Grain-size-dependent remanence anisotropy and its implications for paleodirections and paleointensities—proposing a new approach to anisotropy corrections, *Earth planet. Sci. Lett.*, **512**, 111–123.
- Biedermann, A.R., Jackson, M., Bilardello, D. & Feinberg, J.M., 2019b.
 Anisotropy of full and partial anhysteretic remanence across different rock types: 2. Coercivity-dependence of remanence anisotropy, *Tectonics*, under review.
- Biedermann, A.R., Jackson, M., Stillinger, M.D., Bilardello, D. & Feinberg, J.M., 2019c. Anisotropy of full and partial anhysteretic remanence across different rock types: 1. Are partial anhysteretic remanence anisotropy tensors additive?, *Tectonics*, under review.
- Bilardello, D., 2015. Isolating the anisotropy of the characteristic remanencecarrying hematite grains: a first multispecimen approach, *Geophys. J. Int.*, **202**, 695–712.
- Bilardello, D. & Jackson, M.J., 2014. A comparative study of magnetic anisotropy measurement techniques in relation to rock-magnetic properties, *Tectonophysics*, **629**, 39–54.
- Bilardello, D. & Kodama, K.P., 2009. Measuring remanence anisotropy of hematite in red beds: anisotropy of high-field isothermal remanence magnetization (hf-AIR), *Geophys. J. Int.*, **178**, 1260–1272.
- Bilardello, D. & Kodama, K.P., 2010. A new inclination shallowing correction of the Mauch Chunk formation of Pennsylvania, based on high-field AIR results: implications for the Carboniferous North American APW path and Pangea reconstructions, *Earth planet. Sci. Lett.*, 299, 218–227.
- Bogue, S.W., Gromme, S. & Hillhouse, J.W., 1995. Paleomagnetism, magnetic anisotropy, and mid-Cretaceous paleolatitude of the Duke island (Alaska) ultramafic complex, *Tectonics*, 14, 1133–1152.
- Borradaile, G.J. & Dehls, J.F., 1993. Regional kinematic inferred from magnetic subfabrics in Archean rocks of Northern Ontario, Canada, *J. Struct. Geol.*, **15**, 887–894.
- Borradaile, G.J. & Henry, B., 1997. Tectonic applications of magnetic susceptibility and its anisotropy, *Earth-Sci. Rev.*, 42, 49–93.
- Borradaile, G.J. & Jackson, M., 2010. Structural geology, petrofabrics and magnetic fabrics (AMS, AARM, AIRM), J. Struct. Geol., 32, 1519–1551.
- Cagnoli, B. & Tarling, D., 1997. The reliability of anisotropy of magnetic susceptibility (AMS) data as flow direction indicators in friable base surge and ignimbrite deposits: Italian examples, *J. Volc. Geotherm. Res.*, 75, 309–320.
- Coe, R.S., 1966. Analysis of magnetic shape anisotropy using second-rank tensors, *J. geophys. Res.*, **71**, 2637–2644.
- Cox, A. & Doell, R.R., 1967. Measurement of high-coercivity magnetic anisotropy, in Methods in Palaeomagnetism, pp. 477–482, eds Collinson, D.W., Creer, K.M. & Runcorn, S.K., Elsevier.
- Crameri, F., 2018. Geodynamic diagnostics, scientific visualisation and StagLab 3.0, Geoscientific Model Dev. Discuss., 11, 2541–2562.
- de Wall, H., 2000. The field dependence of AC susceptibility in titanomagnetites: implications for the anisotropy of magnetic susceptibility, Geophys. Res. Lett., 27, 2409–2411.

- de Wall, H. & Worm, H.-U., 1993. Field dependence of magnetic anisotropy in pyrrhotite: effects of texture and grain shape, *Phys. Earth planet. Inter.*, **76**, 137–149.
- di Capua, A., 2014, Volcanism versus tectonics in the sedimentary record, *PhD thesis*, Universita degli study di Milano-Bicocca.
- Feinberg, J.M., Wenk, H.-R., Scott, G.R. & Renne, P.R., 2006. Preferred orientation and anisotropy of seismic and magnetic properties in gabbronorites from the Bushveld layered intrusion, *Tectonophysics*, 420, 345–356.
- Font, E., Trindade, R.I.F. & Nédélec, A., 2005. Detrital remanent magnetization in haematite-bearing Neoproterozoic Puga cap dolostone, Amazon craton: a rock magnetic and SEM study, *Geophys. J. Int.*, 163, 491–500.
- Garrick-Bethell, I., Weiss, B.P., Shuster, D.L., Tikoo, S.M. & Tremblay, M.M., 2016. Further evidence for early lunar magnetism from troctolite 76535, J. geophys. Res., 121, doi:10.1002/2016JE005154.
- Girdler, R.W., 1961. The measurement and computation of anisotropy of magnetic susceptibility in rocks, Geophys. J. R. astr. Soc., 5, 34–44.
- Guerrero-Suarez, S. & Martin-Hernandez, F., 2012. Magnetic anisotropy of hematite natural crystals: increasing low-field strength experiments, *Int.* J. Earth Sci., 101, 625–636.
- Henry, B. & Daly, L., 1983. From qualitative to quantitative magnetic anisotropy analysis: the prospect of finite strain calibration, *Tectonophysics*, 98, 327–336.
- Hext, G.R., 1963. The estimation of second-order tensors, with related tests and designs, *Biometrika*, **50**, 353–373.
- Hillhouse, J.W., 2010. Clockwise rotation and implications for northward drift of the western Transverse Ranges from paleomagnetism of the Piuma Member, Sespe Formation, near Malibu, California, Geochem. Geophys. Geosyst., 11, Q07005, doi:10.1029/2010GC003047.
- Hodych, J.P. & Buchan, K.L., 1994. Early Silurian palaeolatitude of the Springdale group redbeds of central Newfoundland: a palaeomagnetic determination with a remanence anisotropy test for inclination error, *Geophys. J. Int.*, 117, 640–652.
- Hrouda, F., 1982. Magnetic anisotropy of rocks and its application in geology and geophysics, Geophys. Surv., 5, 37–82.
- Hrouda, F., 1986. The effect of quartz on the magnetic anisotropy of quartzite, Stud. Geophys. Geod., 30, 39–45.
- Hrouda, F., 2002a. Low-field variation of magnetic susceptibility and its effect on the anisotropy of magnetic susceptibility of rocks, *Geophys. J. Int.*, 150, 715–723.
- Hrouda, F., 2002b. The use of the anisotropy of magnetic remanence in the resolution of the anisotropy of magnetic susceptibility into its ferromagnetic and paramagnetic components, *Tectonophysics*, **347**, 269–281.
- Hrouda, F., 2004. Problems in interpreting AMS parameters in diamagnetic rocks, in *Magnetic Fabric: Methods and Applications*, pp. 49–59, eds Martín-Hernández, F., Lüneburg, C.M., Aubourg, C. & Jackson, M., The Geological Society.
- Hrouda, F., 2009. Determination of field-independent and field-dependent components of anisotropy of susceptibility through standard AMS measurement in variable low fields I: theory, *Tectonophysics*, 466, 114–122.
- Hrouda, F., Henry, B. & Borradaile, G.J., 2000. Limitations of tensor subtraction in isolating diamagnetic fabrics by magnetic anisotropy, *Tectonophysics*, 322, 303–310.
- Hrouda, F., Chadima, M. & Jezek, J., 2018. Anisotropy of susceptibility in rocks which are magnetically nonlinear even in low fields, *Geophys. J. Int.*, 213, 1792–1803.
- Jackson, M., 1991. Anisotropy of magnetic remanence: a brief review of mineralogical sources, physical origins, and geological applications, and comparison with susceptibility anisotropy, *Pure appl. Geophys.*, 136, 1– 28.
- Jackson, M. & Borradaile, G., 1991. On the origin of the magnetic fabric in purple Cambrian slates of North Wales, *Tectonophysics*, **194**, 49–58.
- Jackson, M. & Tauxe, L., 1991. Anisotropy of magnetic susceptibility and remanence: developments in the characterization of tectonic, sedimentary, and igneous fabric, *Rev. Geophys.*, 29, 371–376.
- Jackson, M., Gruber, W., Marvin, J. & Banerjee, S.K., 1988. Partial anhysteretic remanence and its anisotropy: applications and grainsizedependence, *Geophys. Res. Lett.*, 15, 440–443.

- Jackson, M., Sprowl, D. & Ellwood, B., 1989. Anisotropies of partial anhysteretic remanence and susceptibility in compacted black shales: grainsize-and composition-dependent magnetic fabric, *Geophys. Res. Lett.*, 16, 1063–1066
- Jackson, M., Moskowitz, B., Rosenbaum, J. & Kissel, C., 1998. Field-dependence of AC susceptibility in titanomagnetites, *Earth planet. Sci. Lett.*, 157, 129–139.
- Jelinek, V., 1977. The Statistical Theory of Measuring Anisotropy of Magnetic Susceptibility of Rocks and its Application, Geofyzika, Brno, Czech Republic.
- Jelinek, V., 1981. Characterization of the magnetic fabric of rocks, Tectonophysics, 79, T63-T67.
- Jelinek, V., 1984. On a mixed quadratic invariant of the magnetic susceptibility tensor, J. Geophys., 56, 58–60.
- Johns, M.K., Jackson, M.J. & Hudleston, P.J., 1992. Compositional control of magnetic anisotropy in the Thomson formation, east-central Minnesota, *Tectonophysics*, 210, 45–58.
- Kodama, K.P. & Dekkers, M.J., 2004. Magnetic anisotropy as an aid to identifying CRM and DRM in red sedimenetary rocks, *Stud. Geophys. Geod.*, 48, 747–766.
- Kovacheva, M., Chauvin, A., Jordanova, N., Lanos, P. & Karloukovski, V., 2009. Remanence anisotropy effect on the palaeointensity results obtained from various archaeological materials, excluding pottery, *Earth Planets Space*, 61, 711–732.
- Lawrence, R.M., Gee, J.S. & Karson, J.A., 2002. Magnetic anisotropy of serpentinized peridotites from the MARK area: implications for the orientation of mesoscopic structures and major fault zones, *J. geophys. Res.*, 107, 2073, doi:10.1029/2000JB000007.
- Lu, G. & McCabe, C., 1993. Magnetic fabric determined from ARM and IRM anisotropies in Paleozoic carbonates, southern Appalachian Basin, Geophys. Res. Lett., 20, 1099–1102.
- Lycka, R., 2017, A systematic comparison of the anisotropy of magnetic susceptibility (AMS) and anisotropy of remanence (ARM) fabrics of ignimbrites: examples from the quaternary Bandelier Tuff, Jemez Mountains, New Mexico and Miocene ignimbrites near Gold Point, Nevada, *PhD thesis*, University of Texas.
- Martín-Hernández, F. & Ferré, E.C., 2007. Separation of paramagnetic and ferrimagnetic anisotropies: a review, *J. geophys. Res.*, 112, doi:10.1029/2006JB004340.
- Martín-Hernández, F., Lüneburg, C.M., Aubourg, C. & Jackson, M., 2004.
 Magnetic Fabrics: Methods and Applications, Vol. 238, The Geological Society.
- Maxbauer, D.P., Feinberg, J.M. & Fox, D.L, 2016. MAX UnMix: a web application for unmixing magnetic coercivity distributions, *Comput. Geosci.*, 95, 140–145.
- McCabe, C., Jackson, M.J. & Ellwood, B.B., 1985. Magnetic anisotropy in the Trenton limestone: results of a new technique, anisotropy of anhysteretic susceptibility, *Geophys. Res. Lett.*, 12, 333–336.
- McCall, A.M. & Kodama, K.P., 2014. Anisotropy-based inclination correction for the Moenave formation and Wingate sandstone: implications for Colorado Plateau rotation, *Frontiers Earth Sci.*, 2, 15, doi:10.3389/feart.2014.00015.
- McEnroe, S.A., Robinson, P. & Panish, P.T., 2001. Aeromagnetic anomalies, magnetic petrology, and rock magnetism of hemo-ilmenite- and magnetite-rich cumulate rocks from the Sokndal region, south Rogaland, Norway, Am. Mineral., 86, 1447–1468.
- Mitra, R., Tauxe, L. & Gee, J.S., 2011. Detecting uniaxial single domain grains with a modified IRM technique, *Geophys. J. Int.*, **187**, 1250–1258.
- Mitra, R., Tauxe, L. & Gee, J.S., 2012. Reply to the comment by K. Fabian on 'Detecting uniaxial single domain grains with a modified IRM technique', Geophys. J. Int., 191, 46–50.
- Owens, W.H., 1974. Mathematical model studies on factors affecting the magnetic anisotropy of deformed rocks, *Tectonophysics*, 24, 115–131.
- Pariso, J.E. & Johnson, H.P., 1993. Do lower crustal rocks record reversals of the Earth's magnetic field? Magnetic petrology of oceanic gabbros from ocean drilling program hole 735B, J. geophys. Res., 98, 16013–16032.
- Potter, D.K., 2004. A comparison of anisotropy of magnetic remanence methods—a user's guide for application to paleomagnetism and magnetic

- fabric studies, in *Magnetic Fabrics: Methods and Applications*, pp. 21–35, eds Martín-Hernández, F., Lüneburg, C.M., Aubourg, C. & Jackson, M., The Geological Society.
- Raposo, M.I.B., D'Agrella-Filho, M.S. & Siqueira, R., 2003. The effect of magnetic anisotropy on paleomagnetic directions in high-grade metamorphic rocks from the Juiz de Fora Complex, SE Brazil, *Earth planet. Sci. Lett.*, 209, 131–147.
- Raposo, M.I.B., Chaves, A.O., Lojkasek-Lima, P., D'Agrella-Filho, M.S. & Teixeira, W., 2004. Magnetic fabrics and rock magnetism of Proterozoic dike swarm from the southern Sao Francisco Craton, Minas Gerais State, Brazil, *Tectonophysics*, 378, 43–63.
- Roberts, A.P., 2006. High-resolution magnetic analysis of sediment cores: strengths, limitations and strategies for maximizing the value of long-core magnetic data, *Phys. Earth planet. Inter.*, **156**, 162–178.
- Rochette, P., Jackson, M. & Aubourg, C., 1992. Rock magnetism and the interpretation of anisotropy of magnetic susceptibility, Rev. Geophys., 30, 209–226
- Selkin, P.A., Gee, J.S., Tauxe, L., Meurer, W.P. & Newell, A.J., 2000. The effect of remanence anisotropy on paleointensity estimates: a case study from the Archean Stillwater Complex, *Earth planet. Sci. Lett.*, **183**, 403– 416.
- Stephenson, A., Sadikun, S. & Potter, D.K., 1986. A theoretical and experimental comparison of the anisotropies of magnetic susceptibility and remanence in rocks and minerals, *Geophys. J. R. astr. Soc.*, 84, 185–200.
- Stokking, L.B. & Tauxe, L., 1990. Properties of chemical remanence in synthetic hematite: testing theoretical predictions, *J. geophys. Res.*, 95, 12 639–12 652.
- Sun, W., Hudleston, P.J. & Jackson, M., 1995. Magnetic and petrographic studies in the multiply deformed Thomson formation, east-central Minnesota, *Tectonophysics*, 249, 109–124.
- Tamaki, M. & Itoh, Y., 2008. Tectonic implications of paleomagnetic data from upper cretaceous sediments in the Oyubari area, central Hokkaido, Japan, *Island Arc*, 17, 270–284.
- Tan, X. & Kodama, K., 2002. Magnetic anisotropy and paleomagnetic inclination shallowing in red beds: evidence from the Mississippian Mauch Chunk formation, Pennsylvania, *J. geophys. Res.*, 107, doi:10.1029/2001JB001636.
- Tan, X., Kodama, K.P., Chen, H., Fang, D., Sun, D. & Li, Y., 2003. Paleomagnetism and magnetic anisotropy of cretaceous red beds from the Tarim

- Basin, northwest China: evidence for a rock magnetic cause of anomalously shallow paleomagnetic inclinations from central Asia, *J. geophys. Res.*, **108**, 2107, doi:10.1029/2001JB001608.
- Tarling, D.H. & Hrouda, F., 1993. *The Magnetic Anisotropy Rocks*, Chapman and Hall.
- Tauxe, L., Constable, C., Stokking, L. & Badgley, C., 1990. Use of anisotropy to determine the origin of characteristic remanence in the Siwalik red beds of northern Pakistan, J. geophys. Res., 95, 4391–4404.
- Tema, E., 2009. Estimate of the magnetic anisotropy effect on the archaeomagnetic inclination of ancient bricks, *Phys. Earth planet. Inter.*, 176, 213–223.
- Tikoo, S.M., Weiss, B.P., Buz, J., Lima, E.A., Shea, E.K., Melo, G. & Grove, T.L., 2012. Magnetic fidelity of lunar samples and implications for an ancient core dynamo, *Earth planet. Sci. Lett.*, 337–338, 93–103.
- Trindade, R.I.F., Bouchez, J.-L., Bolle, O., Nédélec, A., Peschler, A. & Poitrasson, F., 2001. Secondary fabrics revealed by remanence anisotropy: methodological study and examples from plutonic rocks, *Geophys. J. Int.*, 147, 310–318.
- Usui, Y., Nakamura, N. & Yoshida, T., 2006. Magnetite microexsolutions in silicate and magmatic flow fabric of the Goyozan granitoid (NE Japan): significance of partial remanence anisotropy, *J. geophys. Res.*, 111, B11101, doi:10.1029/2005JB004183.
- Worm, H.-U., 1991. Multidomain susceptibility and anomalously strong low field dependence of induced magnetization in pyrrhotite, *Phys. Earth planet. Inter.*, **69**, 112–118.
- Yu, Y., Dunlop, D.J. & Özdemir, Ö., 2002. Partial anhysteretic remanent magnetization in magnetite—1. Additivity, *J. geophys. Res.*, **107**, 2244, doi:10.1029/2001JB001249.

SUPPORTING INFORMATION

Supplementary data are available at *GJI* online.

 $Table A_IRMacqu_unmixing.xlsx$

TableB_AIRM.xlsx

Please note: Oxford University Press are not responsible for the content or functionality of any supporting materials supplied by the authors. Any queries (other than missing material) should be directed to the corresponding author for the paper.